Inverse Problem in Anisotropic Poroelasticity: Drained Constants from Undrained Ultrasound Measurements

James G. Berryman and Seiji Nakagawa

Earth Sciences Division,

Lawrence Berkeley National Laboratory,

One Cyclotron Road MS90-R1116,

Berkeley,

CA 94720,

USA.

(Dated: November 20, 2009)

Abstract

Poroelastic analysis has traditionally focused on the relationship between dry or drained constants which are assumed known and the saturated or undrained constants which are assumed unknown. However, there are many applications in this field of study for which the main measurements can only be made on the saturated/undrained system, and then it is uncertain what the effects of the fluids were on the system, since the drained constants remain a mystery. The work presented here shows how to deduce drained constants from undrained constants for anisotropic systems having symmetries ranging from isotropic to orthotropic. Laboratory ultrasound data are then inverted for the drained constants in three granular packings: one of glass beads, and two others for distinct types of more or less angular sand grain packings. Experiments were performed under uniaxial stress, which resulted in hexagonal (transversely isotropic) symmetry of the poroelastic response. One important conclusion from the general analysis is that the drained constants are uniquely related to the undrained constants, assuming that porosity, grain bulk modulus, and pore fluid bulk modulus are already known. Since the resulting system of equations for all the drained constants is linear, measurement error in undrained constants also propagates linearly into the computed drained constants.

PACS numbers: 43.30.Ma,43.30.Pc

I. INTRODUCTION

Analysis of poroelastic systems typically focuses on how poroelastic moduli from measurements of undrained samples are related to the pore-fluid and drained system elastic properties.[1] These technical terms in poroelasticity sometimes have slightly different names and meanings throughout the literature, but the approximate correspondence follows this recipe: undrained $\simeq$ jacketed $\simeq$ unrelaxed, while drained $\simeq$ relaxed, and unjacketed $\simeq$ solid $\simeq$ mineral. There are many useful and pertinent references.[2–13] But the inverse problem of deducing drained properties from undrained properties has seldom been addressed by analytical means.[14,15] Nevertheless, this important issue arises many times, especially in oil and gas reservoir field measurements, because it may not be practical to determine the drained moduli separately as it is typically impossible to drain the system — at least over the timescales when this information would be most useful. Another example is that of ocean sediment measurements made in place,[5,12,16] and similarly in soil fluidization during earthquakes.[17,18] Further examples include medical applications, particularly studies of bone and osteoporosis.[19,20]

One purpose of the present work is therefore to show how to deduce these hard-to-measure drained quantities from the easier-to-measure undrained moduli, without requiring the fairly common (but always tedious and uncertain) iterative and/or fitting techniques that are typically used for such purposes at the present time.

We begin by discussing isotropic systems and then progress to orthotropic systems. We ultimately concentrate on transversely isotropic ones as these are the ones for which we currently have laboratory ultrasound data to invert.

II. POROUS MATERIALS CONTAINING FLUIDS

We first consider isotropic and microhomogeneous elastic materials containing voids or pores, where the pores are connected (having finite permeability) and fluid-filled. This situation is the one originally studied by Gassmann.[21] One simplification that arises imme-

diately is due to the fact that the presence of pore fluids — in microhomogeneous and overall isotropic porous media[11,21] — has no mechanical effect on shear moduli that are not coupled to the principal stresses, so $\mu^u = \mu^d$, which means that the undrained ("u" superscript) shear modulus is the same as the drained ("d" superscript) shear modulus, for the overall porous system. There can be (and often may be in practice) other effects on the shear moduli due to the presence of pore fluids, such as softening of cementing materials or expansion of interstitial clays, which we shall term "chemical" effects to distinguish them from the purely mechanical effects to be considered here. We neglect all such chemical effects in the following analysis. This means that mechanical and acoustical analysis for the effective shear moduli is typically unaltered by the presence of fluids.[22] Thus, we may simplify our system of equations in order to focus only on those significant parts of the analysis, *i.e.*, the ones that change due to the mechanical properties of the pore fluids.

A. Isotropy

We start the analysis by showing Gassmann's equation,[21] which for isotropic systems is sometimes written in the following form:

$$K^u = K^d + \alpha^2/[(\alpha - \phi)/K_s + \phi/K_f], \tag{1}$$

where $\alpha \equiv 1 - K^d/K_s$ is the effective stress or Biot-Willis coefficient,[4] K_s is the solid modulus of the grains (assumed to be a homogeneous collection composed of grains of the same mineral), K_f is the fluid modulus, and ϕ is the porosity. Now, by introducing a modulus for a fluid suspension having the same solid and fluid components, but the corresponding drained modulus is $K^d \equiv 0$, we find that the effective modulus is given by

$$K_{susp} = \left[\frac{1-\phi}{K_s} + \frac{\phi}{K_f}\right]^{-1}. \tag{2}$$

In fact this result follows directly from Gassmann's formula by setting $K^d = 0$ everywhere in (1). But of course it is also a well-known exact result[23] in mechanics and acoustics for these types of fluid-solid suspensions.

Rewriting Gassmann's formula in these terms, we find first that

$$K^u = K^d + \frac{(1 - K^d/K_s)^2}{1/K_{susp} - K^d/K_s^2}. \tag{3}$$

Now if we simply multiply through by the denominator on the right hand side, we find

$$K^u \left(\frac{1}{K_{susp}} - \frac{K^d}{K_s^2} \right) = 1 - 2\frac{K^d}{K_s} + \frac{K^d}{K_{susp}}. \tag{4}$$

Note that two terms of the form $(K^d/K_s)^2$ have cancelled from this expression. Once these convenient cancellations have occurred, K^d now appears only linearly in this expression. The equation can therefore be solved immediately for K^d in terms of the undrained modulus K^u and the other factors that are also assumed to be known (and in fact these other factors are typically easier to measure than either K^u or K^d). Finally, we find:

$$K^d = \left(\frac{K^u}{K_{susp}} - 1 \right) \left[1/K_{susp} - 2/K_s + K^u/K_s^2 \right]^{-1}. \tag{5}$$

This form is very useful in our present applications, but so far it applies only to the fully isotropic case. We show next that a very similar (but nevertheless distinct) formula applies to the anisotropic cases under consideration here. This version of the formula (for the isotropic case only) has been derived previously by Zhu and McMechan[14,15]

B. Orthotropy

If the overall porous medium is anisotropic either due to some preferential alignment of the constituent particles or due to externally imposed stress (such as a gravity field and weight of overburden, for example), we consider the orthorhombic anisotropic version of the poroelastic equations:

$$\begin{pmatrix} e_{11} \\ e_{22} \\ e_{33} \\ -\zeta \end{pmatrix} = \begin{pmatrix} s_{11} & s_{12} & s_{13} & -\beta_1 \\ s_{12} & s_{22} & s_{23} & -\beta_2 \\ s_{13} & s_{23} & s_{33} & -\beta_3 \\ -\beta_1 & -\beta_2 & -\beta_3 & \gamma \end{pmatrix} \begin{pmatrix} \sigma_{11} \\ \sigma_{22} \\ \sigma_{33} \\ -p_f \end{pmatrix}. \tag{6}$$

The e_{ii} are strains in the $i = 1, 2, 3$ directions. The σ_{ii} are the corresponding stresses. The fluid pressure is p_f. The increment of fluid content is ζ. The drained compliances are $s_{ij} = s^d_{ij}$. Undrained compliances (not yet shown) are symbolized by s^u_{ij}. Coefficients $\beta_i = s_{i1} + s_{i2} + s_{i3} - 1/3K_s$, where K_s is again the solid modulus of the grains (assumed uniform for simplicity here). The Reuss average bulk modulus[24,25] is defined by

$$\frac{1}{K^d_R} = \sum_{ij=1,2,3} s^d_{ij}. \tag{7}$$

A similar definition of K^u_R, with undrained compliances replacing drained compliances, will also be needed later in our discussion. The alternative Voigt average[25,26] of the stiffnesses ($K^d_V = \sum_{ij=1,2,3} c^d_{ij}/9$) will play no significant role in our present discussion, although we will show some of these values later with the examples. And, finally, $\gamma = \sum_{i=1-3} \beta_i / BK^d_R$, where B is Skempton's coefficient,[27] which will be defined carefully later in our discussion.

The shear terms due to twisting motions (*i.e.*, strains e_{23}, e_{31}, e_{12} and stresses σ_{23}, σ_{31}, σ_{12}) are excluded from the present discussion since they typically do not couple to the modes of interest for anisotropic systems having orthotropic symmetry, or any still more symmetric system such as transversely isotropic or isotropic. We have also assumed that we know the true axes of symmetry, and have made use of them in our formulation of the problem; this helps to eliminate coupling between the modes shown here and those shear modes not displayed (which can happen for systems less symmetric than orthorhombic). Note that the s_{ij}'s are the elements of the compliance matrix $\mathbf{S}$ and are all independent of the fluid, and therefore would be the same if the medium were treated as elastic (*i.e.*, by ignoring the fluid pressure, or assuming that the fluid saturant is air). We typically call these compliances the drained compliances and the corresponding matrix the drained compliance matrix $\mathbf{S}^d$, since the fluids do not contribute to the mechanical energy if they are free to drain into a surrounding reservoir containing the same type of fluid. In contrast, the undrained compliance matrix $\mathbf{S}^u$ presupposes that the fluid is trapped (unable to drain from the system into an adjacent reservoir), and therefore contributes in a significant and measurable way to the compliance and stiffness ($\mathbf{C}^u = [\mathbf{S}^u]^{-1}$) of the undrained system.

The poroelasticity matrix in (6) is in compliance form and has extremely simple poroelastic behavior in the sense that *all the fluid mechanical effects* appear only in the single coefficient γ. We can simplify the notation a little more by lumping some coefficients together, combining the 3×3 submatrix in the upper left corner of the matrix in (6) into $\mathbf{S}$, and defining the column vector $\mathbf{b}$ by

$$\mathbf{b}^T \equiv (\beta_1, \beta_2, \beta_3). \tag{8}$$

The resulting 4×4 matrix and its inverse are now related by:

$$\begin{pmatrix} \mathbf{S} & -\mathbf{b} \\ -\mathbf{b}^T & \gamma \end{pmatrix} = \begin{pmatrix} \mathbf{A} & \mathbf{q} \\ \mathbf{q}^T & z \end{pmatrix}^{-1}, \tag{9}$$

where the elements of the inverse matrix can be shown to be written in terms of drained stiffness matrix $\mathbf{C}^d = \mathbf{C} = \mathbf{S}^{-1}$ by introducing three components: (a) the scalar $z = \left[\gamma - \mathbf{b}^T\mathbf{C}\mathbf{b}\right]^{-1}$, (b) the column vector $\mathbf{q} = z\mathbf{C}\mathbf{b}$, and (c) the undrained 3×3 stiffness matrix (*i.e.*, the pertinent one connecting the principal strains to principal stresses) is given by $\mathbf{A} = \mathbf{C} + z\mathbf{C}\mathbf{b}\mathbf{b}^T\mathbf{C} = \mathbf{C}^d + z^{-1}\mathbf{q}\mathbf{q}^T \equiv \mathbf{C}^u$, since $\mathbf{C}^d$ is the drained stiffness and $\mathbf{A} = \mathbf{C}^u$ is clearly the undrained stiffness by construction.This fact is most easily recognized by noting the inverse relationship, showing that

$$\begin{pmatrix} \mathbf{A} & \mathbf{q} \\ \mathbf{q}^T & z \end{pmatrix} \begin{pmatrix} \mathbf{E} \\ -\zeta \end{pmatrix} = \begin{pmatrix} \mathbf{\Sigma} \\ -p_f \end{pmatrix}, \tag{10}$$

where

$$\mathbf{E} = (e_{11}, e_{22}, e_{33})^T \qquad \text{and} \qquad \mathbf{\Sigma} = (\sigma_{11}, \sigma_{22}, \sigma_{33})^T. \tag{11}$$

When $\zeta = 0$ on the left hand side, the only possible interpretation of the equation is that the nonzero contributions are for the undrained case, and so $\mathbf{A} = \mathbf{C}^u$ is necessarily the undrained stiffness by inspection.

The results contained in (9) and (10) are also equivalent to those of Gassmann[21] for both isotropic and anisotropic porous media as we shall show later in this paper, although Gassmann's results were presented in a form somewhat harder to scan. Also, note the

important fact that the observed decoupling of the fluid effects occurs only in the compliance form (6) of the equations, and never in the stiffness (inverse) form for the poroelasticity equations, since all terms in $\mathbf{A}$, $\mathbf{q}$, and z contain fluid dependent components.

From these results, it is not hard to show that

$$\mathbf{S}^d = \mathbf{S}^u + \gamma^{-1}\mathbf{b}\mathbf{b}^T. \tag{12}$$

This result shows the remarkably simple result that the drained compliance matrix can be found directly from knowledge of the inverse of undrained compliance, and the still unknown, but sometimes relatively easy to estimate, values of γ and the three distinct orthotropic β_i coefficients, for $i = 1, 2, 3$.

Now we make further progress by considering again the Reuss averages of both of the drained and undrained orthotropic compliances:

$$\frac{1}{K_R^d} \equiv s_{11}^d + s_{22}^d + s_{33}^d + 2(s_{12}^d + s_{13}^d + s_{23}^d), \tag{13}$$

and

$$\frac{1}{K_R^u} \equiv s_{11}^u + s_{22}^u + s_{33}^u + 2(s_{12}^u + s_{13}^u + s_{23}^u). \tag{14}$$

These effective moduli are the Reuss averages of the nine compliances in the upper left 3×3 of the full (including the uncoupled shear components) 6×6 compliance matrix for the two cases, respectivley, when the pore fluid is allowed to drain from the porous system, and when the pore fluid is trapped by a jacketing material and therefore undrained.

Although the significance of the formula is somewhat different now, we find again that

$$\beta_1 + \beta_2 + \beta_3 = \frac{1}{K_R^d} - \frac{1}{K_s} = \frac{\alpha_R}{K_R^d} \tag{15}$$

if we also choose to define a Reuss-average effective stress coefficient (or Biot-Willis[4] coefficient) by:

$$\alpha_R \equiv 1 - K_R^d/K_s, \tag{16}$$

in analogy to the isotropic case. Furthermore, we have

$$\gamma = \frac{\beta_1 + \beta_2 + \beta_3}{B} = \frac{\alpha_R}{K_R^d} + \phi\left(\frac{1}{K_f} - \frac{1}{K_s}\right), \tag{17}$$

since we have the rigorous result in this notation (see Berryman[10]) that Skempton's B coefficient is given by

$$B \equiv \frac{1 - K_R^d/K_R^u}{1 - K_R^d/K_s} = \frac{\alpha_R/K_R^d}{\alpha_R/K_R^d + \phi(1/K_f - 1/K_s)}. \tag{18}$$

We emphasize that all these formulas are rigorous statements based on the preceding anisotropic analysis. Note that the appearance of the Reuss averages K_R^d and α_R is not an approximation, but merely a useful choice of notation made here because it will enable us to see clearly the similarity between the rigorous anisotropic formulas and the corresponding isotropic ones.

C. Reuss average moduli

We are now in position to develop the analogy between the isotropic and anisotropic Gassmann equations. In particular, the equation for the suspension modulus in (2) does not change at all. The equation of the effective undrained bulk modulus K^u, as shown in both (1) and (3), changes only in that the relationship is now between the Reuss averages K_R^u and K_R^d of these quantities. The result is completely analogous to (3), and is given for pertinent Reuss average quantities by

$$K_R^u = K_R^d + \frac{(1 - K_R^d/K_s)^2}{1/K_{susp} - K_R^d/K_s^2}. \tag{19}$$

The remainder of the argument is virtually identical to the isotropic case, and the final result for the drained modulus is:

$$K_R^d = \left(\frac{K_R^u}{K_{susp}} - 1\right)\left[1/K_{susp} - 2/K_s + K_R^u/K_s^2\right]^{-1}. \tag{20}$$

This formula shows how to invert for drained Reuss bulk modulus K_R^d from knowledge of K_R^u, ϕ, K_f and K_s in an anisotropic (up to orthotropic) poroelastic system.

Clearly this formula does not yet give us the individual matrix elements s_{ij}^d directly. Nevertheless, (20) was the hardest step in the procedure that follows, and the rest of the steps are easily taken once we have this general result.

First note that, from (15) and (17), it also follows that $\gamma^{-1} = \frac{BK_R^d}{\alpha_R}$. So we can now rearrange (12) to give

$$s_{ij}^d = s_{ij}^u + \frac{BK_R^d}{\alpha_R}\beta_i\beta_j, \quad \text{for} \quad i,j = 1,2,3. \tag{21}$$

At this point in the analysis, we know everything needed for the inversion except for the three coefficients β_i, for $i = 1,2,3$. But, by taking appropriate sums of (21) and recalling Eqn. (15), we find that

$$\beta_i = s_{i1}^d + s_{i2}^d + s_{i3}^d - \frac{1}{3K_s} = s_{i1}^u + s_{i2}^u + s_{i3}^u - \frac{1}{3K_s} + B\beta_i. \tag{22}$$

We used (15) again to show that the product term resulting from (21) is $(K_R^d/\alpha_R)(\beta_1+\beta_2+\beta_3) = 1$. Rearranging (22), we find that

$$\beta_i = \left[s_{i1}^u + s_{i2}^u + s_{i3}^u - \frac{1}{3K_s}\right]/(1-B). \tag{23}$$

Formula (18) for Skempton's coefficient[27] determines B exactly in terms of previously known quantities. So, all three β_i's (which are themselves drained constants) and also γ [using Eqn. (17)] are now precisely determined. All the remaining constants s_{ij}^d can then be found directly from (21). Note that all the steps in this inversion procedure are linear; there is no need to solve any quadratic (or higher order) equation in this formulation of the undrained-to-drained inversion problem. As we shall demonstrate in the examples, it is sufficient to know the c_{ij}^u's, porosity ϕ, and the two bulk moduli K_s and K_f, in order to determine first the β_i's from (23), and then the s_{ij}^d from (21). Once all the s_{ij}^d for all $i,j = 1,2,3$ are known, then the corresponding stiffnesses are found by inverting the pertinent 3×3 matrix of compliances.

III. EXAMPLES

Recently, one of us (together with other colleagues at LBNL[28]) developed a new technology for measuring the seismic/ultrasonic anisotropy of soft sediments during their compaction. This method is based on a specially designed compaction cell, equipped with three

pairs of ultrasonic transducers, including one P-wave and two S-wave transducer pairs. The setup also includes a phased P-wave piezoelectric source array with 32 elements, and a sensor to generate steerable ultrasonic plane waves. The central (or resonance) frequency of the transducers is in the range of 500 kHz–1 MHz. Compared to previously existing methods, this method has the capability (a) to determine all five of the independent elastic constants in a TI (transversely isotropic) medium, (b) to conduct measurements continuously while the sedimentary material is compacted *in situ* (*i.e.*, in the uniaxially pressurized chamber), and (c) does not require single or multiple directionally cored samples (such coring, when needed, actually releases stress of the compacted sediments and therefore does not give accurate measurements of *in situ* conditions). Uniaxial loading was taken to a maximum of 5 MPa.

The spectral content of the measured ultrasonic waves changes significantly during compaction of fluid-saturated sediments. These changes occur primarily because of the scattering of high-frequency acoustic energy, which can be large — particularly for low-velocity S-waves. To reduce the phase-velocity measurement errors related to the changes in the central frequency of the waves, and to reduce the impact of the high-frequency wave scattering in the examples presented in this paper, amplitude spectrum of the measured wave was filtered to have the shape of a Ricker wavelet with a central frequency of 500 kHz for P-waves and 50 kHz for S-waves. From each measurement, the propagation time was determined from the arrival time of a dominant phase (*e.g.*, first peak or trough) compared to the reference measurements (face-to-face measurements of the transducer couples). Four out of the five elastic constants of a TI medium can be determined directly from the wave velocities along the axes of the sample (one P-wave and two S-wave measurements along the horizontal plane, and one P-wave measurement in the vertical direction). The last constant is determined through a numerical inversion method[29] using phase slownesses of the P-waves steered in a range of directions.

Further details of these experimental methods will be presented later in a companion paper. The present work will concentrate on showing examples of the inversion results for

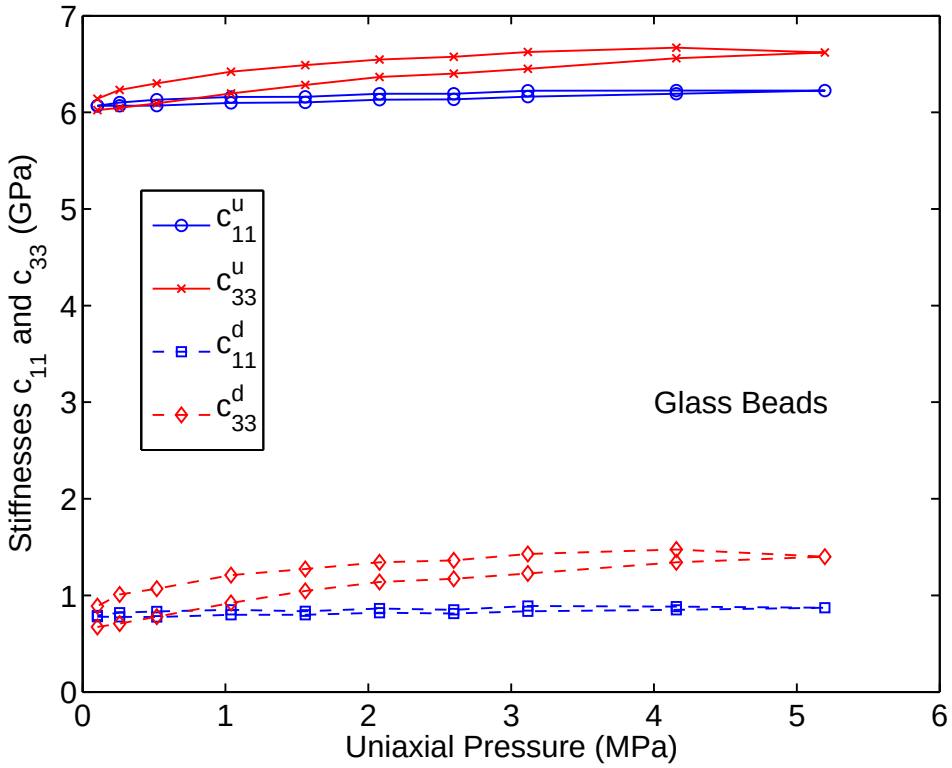

FIG. 1. (color online) Plots of measured undrained (u) and inverted drained (d) constants for the stiffnesses c_{11} and c_{33} in glass bead samples under uniaxial pressure. The abscissa values are those of the uniaxial stress applied to the anisotropic system.

drained constants from the measured values of undrained constants.

A. Examples for transversely isotropic glass bead samples

Experiments were performed on glass bead samples (Potter industry, soda lime glass, size 212 to 250 μm). Figures 1 and 2 display plots of measured undrained (u) and inverted drained (d) constants for stiffnesses obtained by performing ultrasound experiments and measuring the wave speeds in different directions. For example, stiffness $c^u_{33} = \rho v_p^2$, where ρ is the fluid-saturated system density and compressional wave speed v_p is measured along the symmetry axis in our glass bead samples under uniaxial pressure. Figure 1 shows both drained and undrained constants c_{11} and c_{33}, while Figure 2 shows the same types of results

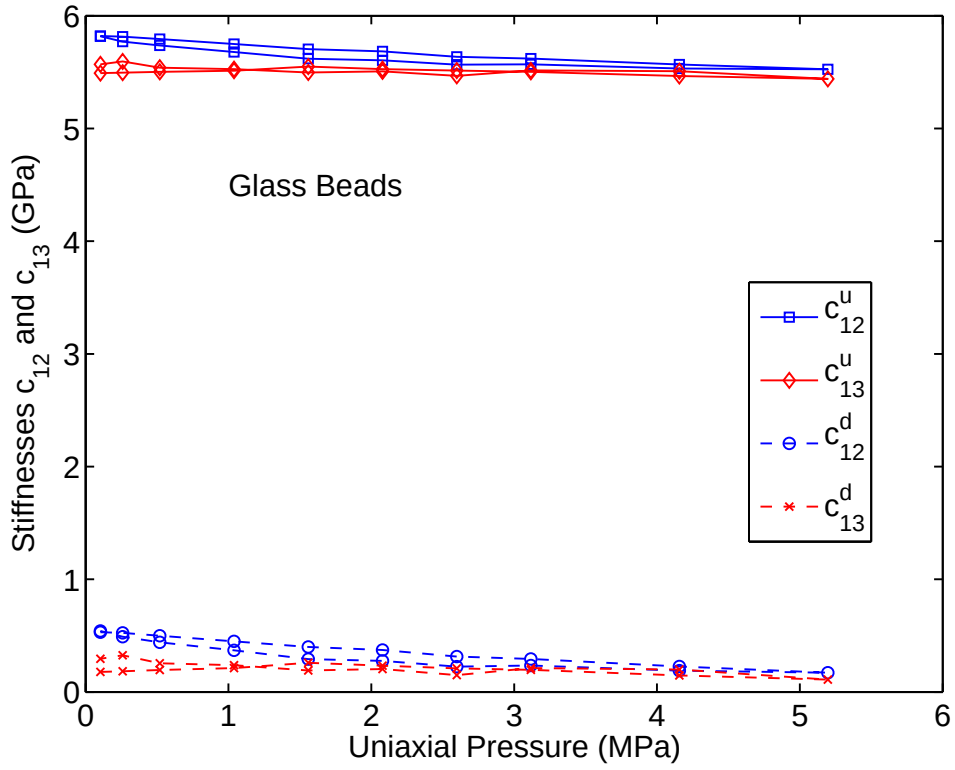

FIG. 2. (color online) Plots of measured undrained (u) and inverted drained (d) constants for the stiffnesses c_{12} and c_{13} in glass bead samples under uniaxial pressure. The abscissa values are the uniaxial stresses applied to the anisotropic system.

for c_{12} and c_{13}. The abscissa values are the applied uniaxial stress. These glass beads had $K_s = 40.7$ GPa, $\mu_s = 29.7$ GPa, and density $\rho_s = 2.46 \times 10^3$ kg/m^3. (For comparison, also see Plona.[30]) Bulk modulus $K_f = 2.2$ GPa for the water saturant. Porosity varied with stress level and was monitored, with values in the range $0.370 \leq \phi \leq 0.375$. Two (or more for the sands) distinct curves are visible for each stiffness as the stress was first cycled up and then down again (repeatedly for the sands), while measurements were made during both (multiple) phases of the test. Figure 3 shows the results for the computed Voigt and Reuss bulk moduli for both measured undrained (K_V^u and K_R^u) and the computed drained cases (K_V^d and K_R^d). Figure 4 shows the measured values of porosity for the cases in Figures 1–3, and also the uniaxial effective stress coefficient X_3. (See Appendix B.)

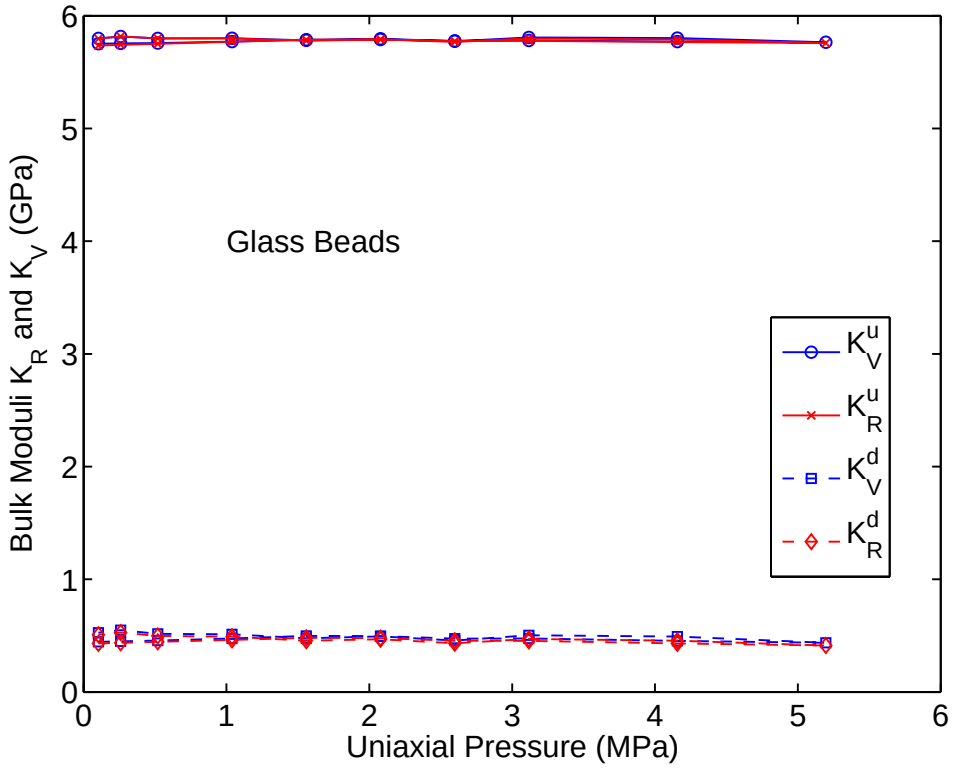

FIG. 3. (color online) For glass bead samples, examples of the undrained and drained bulk modulus estimators K_R and K_V, being the appropriate Reuss and Voigt averages of the compliance and stiffness matrices, respectively. Undrained values were measured, and drained values were computed using the formulas in the text. The drained Voigt averages are found by first computing the drained compliances, then inverting for the drained stiffnesses, and finally averaging. The abscissa values are the uniaxial stresses applied to the anisotropic system. These glass beads had $K_s = 40.7$ GPa, $\mu_s = 29.7$ GPa, and density $\rho_s = 2.46 \times 10^3$ kg/m^3. Bulk modulus $K_f = 2.2$ GPa for water. Porosity varied with stress level and was monitored, with values in the range $0.370 \leq \phi \leq 0.375$.

B. Examples for sand samples: K and OK

The next two sets of Figures follow the same sequencing as that used for presenting the glass bead data. The bulk modulus for the sands was taken as that for quartz, so $K_s = 38.0$ GPa, and $G_s = 44.0$ GPa in both cases. The density of the sand grains was $\rho = 2.65 \times 10^3$

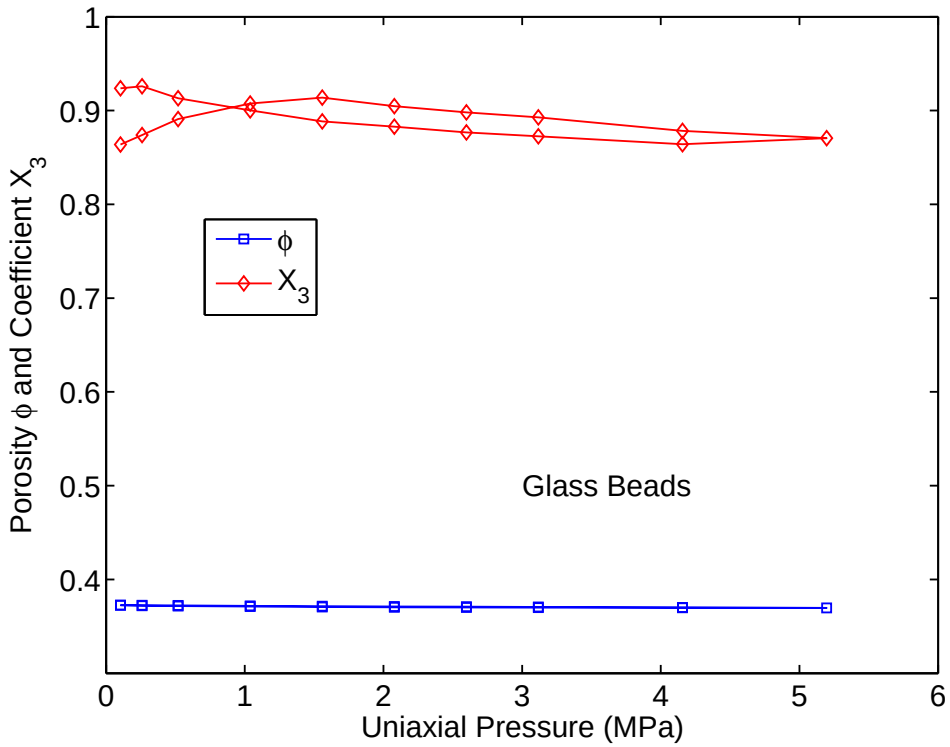

FIG. 4. (color online) Plots of measured porosity ϕ and computed effective uniaxial stress coefficient X_3 in glass bead samples.

kg/m^3. Visual inspection shows that the K sand grains are more angular, and the OK #1 sand grains are significantly less angular. K sand results are presented in Figures 5–8, while those for OK sand are seen in Figures 9–12.

C. Summary of the inversion procedure

The first step of the inversion procedure is to compute the undrained Reuss bulk modulus K_R^u using (14) from measured undrained compliances (or stiffnesess — when these are the measured data as in ultrasound data — by first converting them to compliances). The suspension bulk modulus K_{susp} is also computed from (2) using known values of porosity ϕ, solid grain bulk modulus K_s and pore fluid modulus K_f. These values and K_s again are the only ones needed in formula (20). Once K_R^d is known, then $\alpha_R = 1 - K_R^d/K_s$ is known, and Skempton's coefficient can be computed from (18). Once B is known, then β_1,

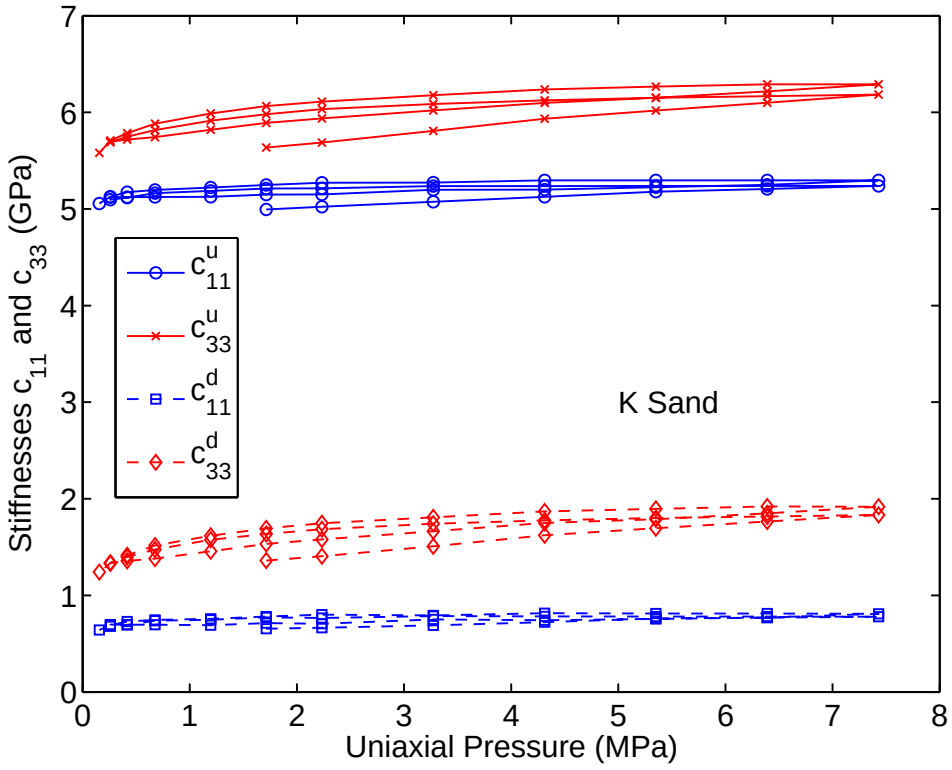

FIG. 5. (color online) Plots of measured undrained (u) and inverted drained (d) constants for the stiffnesses c_{11} and c_{33} in K sand samples under uniaxial pressure. The abscissa values are the uniaxial stresses applied to the anisotropic system.

β_2, and β_3 can all be obtained from (21) and (22). Once all these constants are known, equation (12) is used to compute the individual drained compliance matrix elements. Then, if so desired, the drained stiffness matrix elements may also be computed by inverting the drained compliance matrix. The remaining compliance and stiffness coefficients (*i.e.*, s_{44}, s_{55}, s_{66} — and, therefore, c_{44}, c_{55}, and c_{66}) are not affected by the presence of the fluid, in transversely isotropic (or more generally orthotropic) materials, so their values are the same for both drained and undrained systems.

Also note that the consistently large offset observed between K_R^u and K_R^d is easily understood from the fact that, when $K_R^d << K_s$, Eq. (19) implies

$$K_R^u \simeq K_{susp} + K_R^d, \tag{24}$$

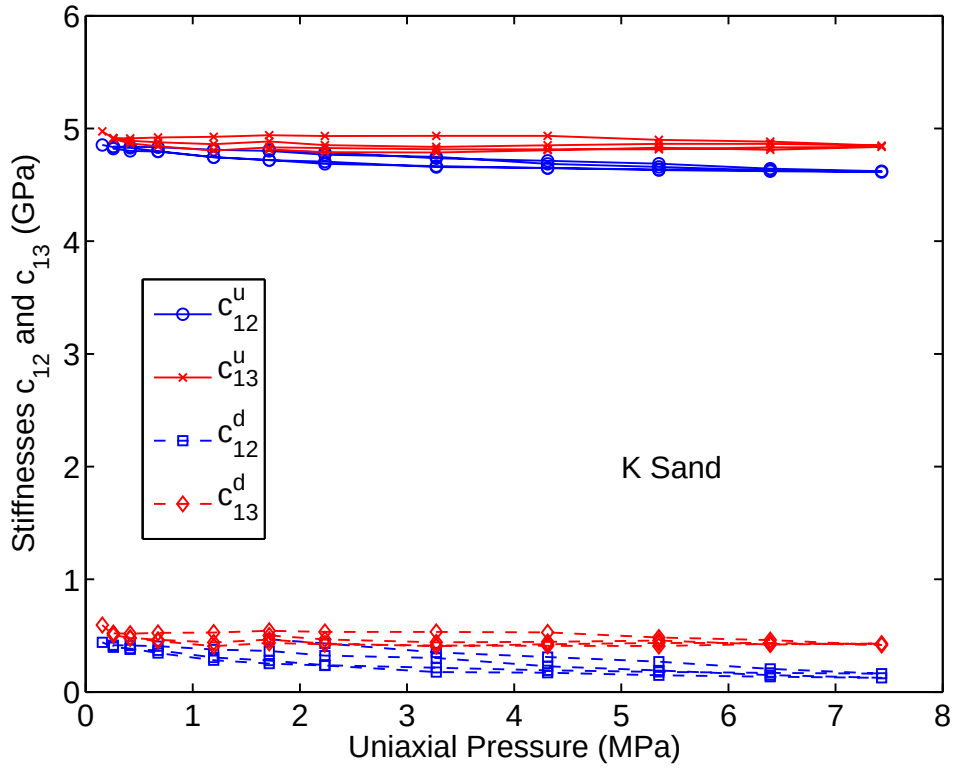

FIG. 6. (color online) Plots of measured undrained (u) and inverted drained (d) constants for the stiffnesses c_{12} and c_{13} in K sand samples under uniaxial pressure. The abscissa numbers are again the computed (true) effective stress values for this anisotropic system. The abscissa values are the uniaxial stresses applied to the anisotropic system.

if we neglect terms of order K_R^d/K_s compared to unity. So the observed offset is almost entirely due to the large value of the suspension modulus K_{susp}, although there are some small corrections of order K_R^d/K_s neglected by (24).

IV. DISCUSSION

The analysis presented in this paper has apparently been wholy quasi-static, treating the stiffnesses and bulk moduli as if they were entirely frequency independent so that Gassmann's quasi-static analysis for either isotropic or anisotropic porous media may be used throughout. The authors are of course well aware of Biot's theory[2,3] of fluid-saturated porous media. This

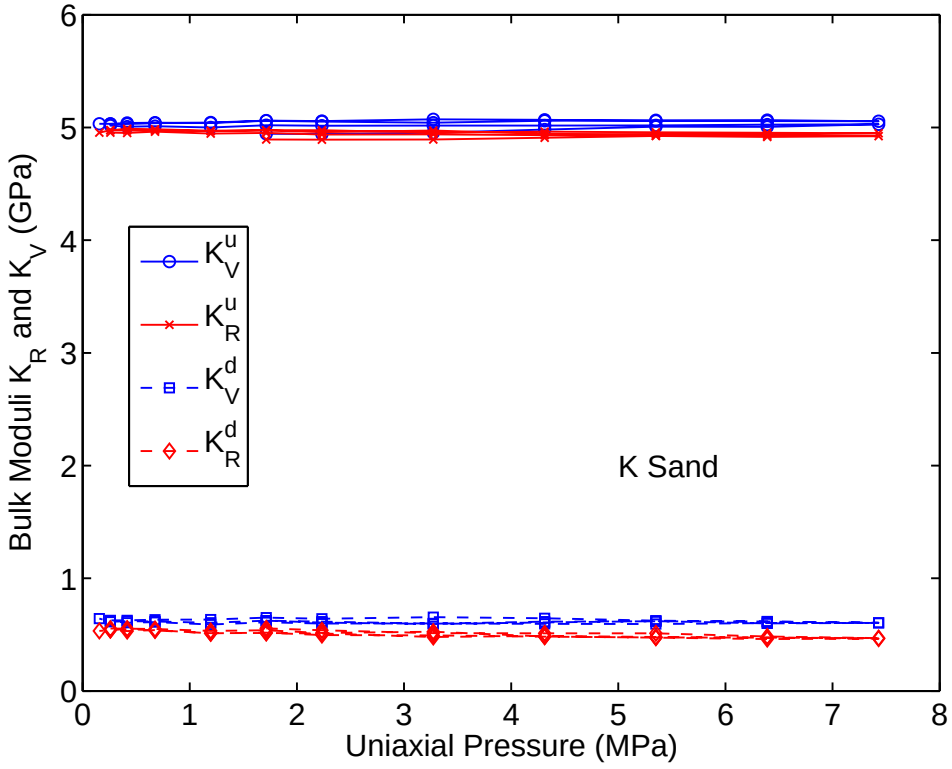

FIG. 7. (color online) For K sand samples, examples of the undrained and drained bulk modulus estimators K_R and K_V, being the appropriate Reuss and Voigt averages of the compliance and stiffness matrices, respectively. The abscissa values are the uniaxial stresses applied to the anisotropic system. These sand grains had $K_s = 38.0$ GPa, $\mu_s = 44.0$ GPa, and density $\rho_s = 2.65 \times 10^3$ kg/m^3. Bulk modulus $K_f = 2.2$ GPa for water. Porosity varied with stress level and was monitored, with values in the range $0.445 \leq \phi \leq 0.480$. Two distinct curves are visible for each stiffness as the stress was first cycled up and then down again, while measurements were made during both phases of the test.

theory introduces the interesting complication of the Biot slow-wave[7,30], which is an out-of-phase motion of the fluid and solid frame that produces strongly fluid-dependent attenuation and scattering mechanisms. Since the experiments that motivated the present work were not designed to measure the attenuation of the resulting waves, and since the very confined nature of the experimental chamber essentially prevents excitation of the Biot slow-wave[31], it seems unnecessary for our present purposes to use the full Biot theory for the analysis.

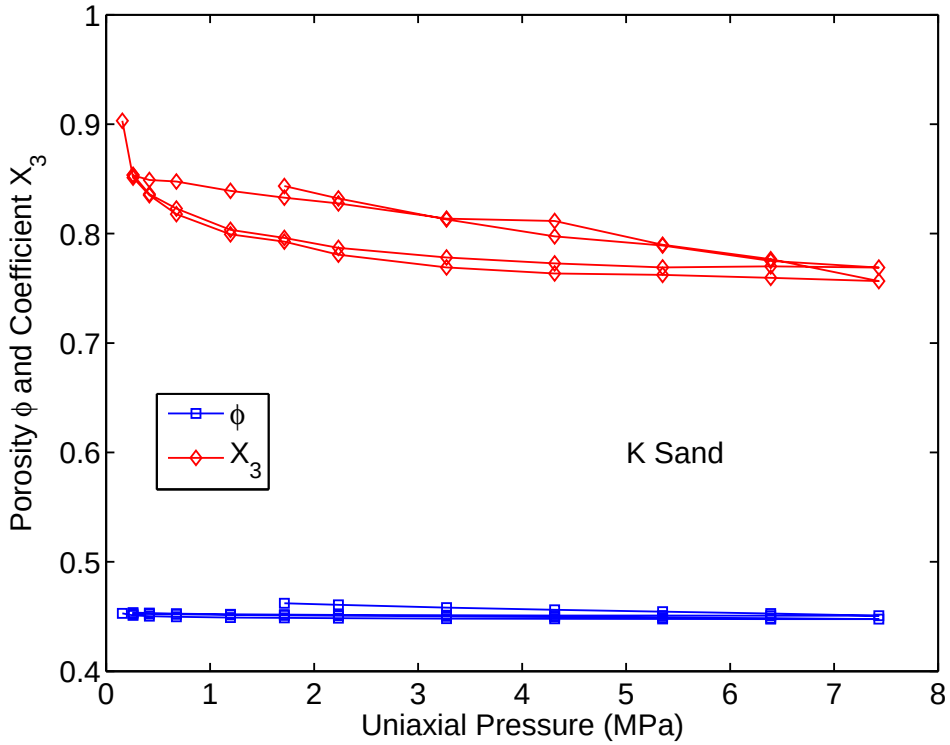

FIG. 8. (color online) Plots of measured porosity ϕ and computed effective uniaxial stress coefficient X_3 in K sand samples.

Thus, we have concentrated instead on the Gassmann approach to the problem.

This treatment does not necessarily imply that frequency plays no role in the experiment. For example, there are good reasons to believe[32] that sometimes an even simpler theory yet, *i.e.*, one treating the frame constants as if they are identically zero, can give a good accounting in some cases of acoustic wave speeds and attenuation in many isotropic granular systems. For present purposes, we view our present work as treating Gassmann's approach as being valid at each fixed frequency – thus making this a viscoelastic theory, rather than just an elastic theory. In the absence of observable slow waves, this approach seems to give a satisfactory approximation to these data. It leads, as we have shown here in detail, to results that allow us to determine effective frame constants of the drained system, valid in the small range of ultrasonic frequencies pertinent to these specific experiments.

We do not assume that these measured values will necessarily hold true for other mea-

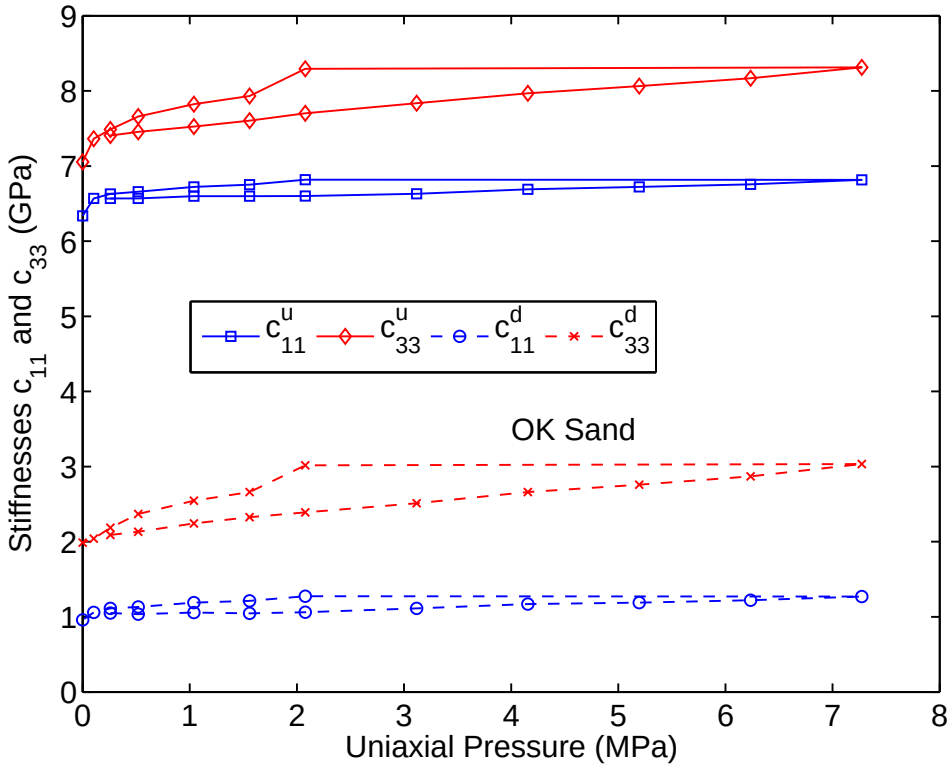

FIG. 9. Plots of measured undrained (u) and inverted drained (d) constants for the stiffnesses c_{11} and c_{33} in OK sand samples under uniaxial pressure. Two distinct curves are visible for each stiffness as the stress was first cycled up and then down again, while measurements were made during both phases of the test. The abscissa values are the uniaxial stresses applied to the anisotropic system.

surements in different frequency bands. In the literature, it is also commonly assumed that there is a small frequency dependent dissipative component associated with these frame constants (see discussion of these issues by Chotiros[33]), but for our present purposes we have treated this dissipative component as negligible, and therefore set it to zero.

V. CONCLUSIONS AND EXTENSIONS

One important conclusion about the general analysis presented here is that the drained constants are uniquely related to the undrained constants, assuming that porosity, grain

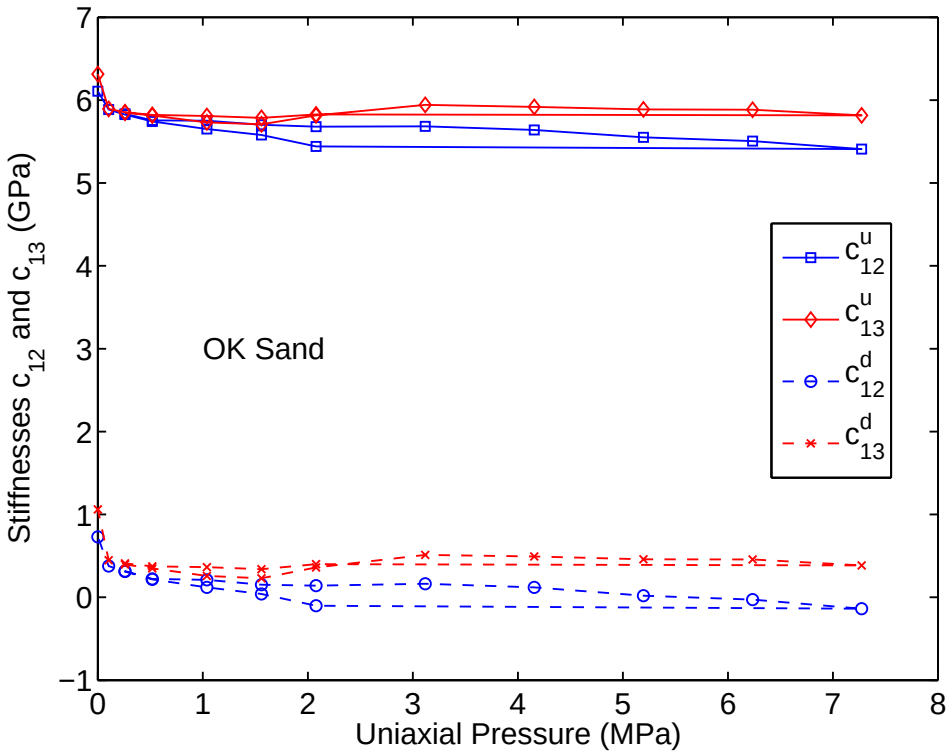

FIG. 10. Plots of measured undrained (u) and inverted drained (d) constants for the stiffnesses c_{12} and c_{13} in OK sand samples under uniaxial pressure. The abscissa values are the uniaxial stresses applied to the anisotropic system.

bulk modulus, and pore-fluid bulk modulus are already known when the porous material is microhomogeneous.[6,21] This fact follows directly from the linearity of the equations being solved. Of course, measurement error in undrained constants and the other constants (porosity, and bulk moduli for grains and pore fluid) is never zero, and so must be taken into account. However, since the equations are linear, the errors also propagate linearly into the computed drained constants. The linearity of this problem also leads to a qualified uniqueness result in the sense that, except for issues already mentioned concerning propagation of measurement errors, the results of the undrained to drained inversion process is unique — in principle. This fact has implications for earlier work that has sometimes been done using fitting or iterative methods, the point being that such methods always have an implicit caveat associated with them that the results found might not be unique (and in

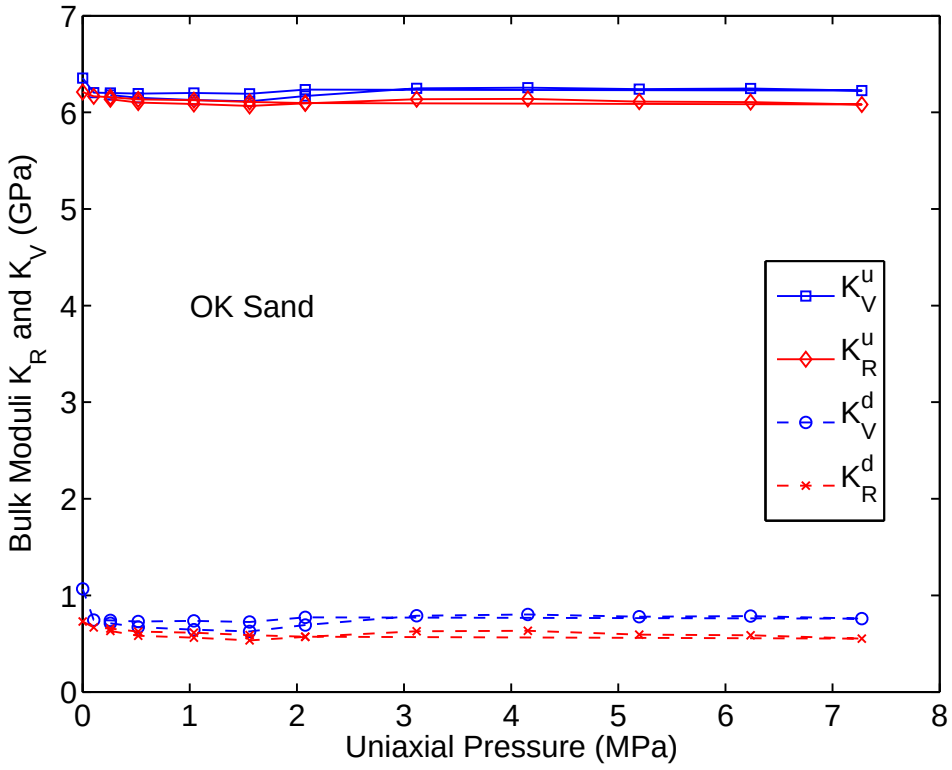

FIG. 11. (color online) For OK sand samples, examples of the undrained and drained bulk modulus estimators K_R and K_V, being the appropriate Reuss and Voigt averages of the compliance and stiffness matrices, respectively. The abscissa values are the uniaxial stresses applied to the anisotropic system. These sand grains had $K_s = 38.0$ GPa, $\mu_s = 44.0$ GPa, and density $\rho_s = 2.65 \times 10^3$ kg/m^3. Bulk modulus $K_f = 2.2$ GPa for water. Porosity varied with stress level and was monitored, with values in the range $0.3496 \leq \phi \leq 0.3502$.

addition they too are obviously subject to the measurement errors) if the system of poroelastic equations happens to have multiple solutions. All that could be said previously of the iterative or fitting methods is that one solution had been found. The present results improve this situation for all such methods since we have shown the solution is actually unique (in principle again, except for the unavoidable measurement errors), and so earlier results of the iterative (or fitting) type may now be assumed to have found good approximations to the (in principle) unique solution of each inversion problem.

One simplification obtained in the chosen range of our analysis is that, since we are

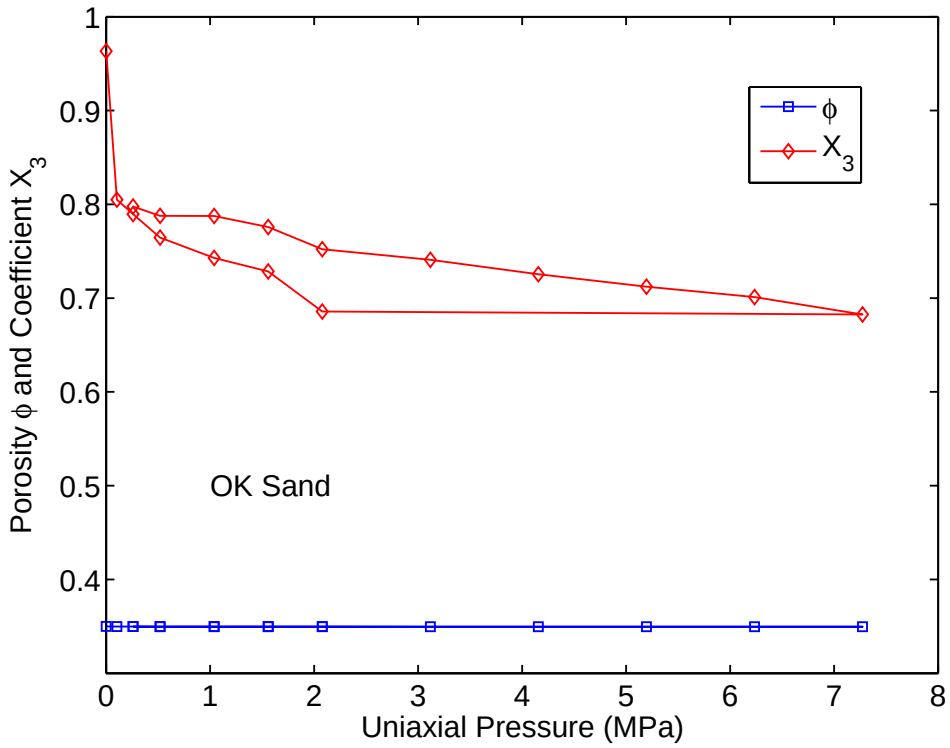

FIG. 12. (color online) Plots of measured porosity ϕ and computed effective uniaxial stress coefficient X_3 in OK sand samples.

specifically considering data on granular materials, we have been able to limit our discussion to ones that happen to be homogeneous mixtures of grains all having the same bulk and shear moduli. This simplification puts our work in the same class as that of Gassmann,[21] Walton,[34] Johnson *et al.*,[35] and many others, including a large number of the laboratory experimental results, including Domenico,[36] Murphy,[37] and Zimmer *et al.*,[38] on granular bead-packs and some sands that are especially homogeneous. We have not tried to deal specifically with issues related to microscopic heterogeneity (other than the pore space itself), but this complication is actually relatively easy to include as needed for such mixed systems[6,39] – the point being that the pertinent generalizations required here involve only Reuss averages of bulk moduli, as we have shown for the simpler cases presented.

Some very general discussions of anisotropic porous media have been given by Thompson and Willis,[40] and Cowin.[41] Both these contributions emphasize the advantages of formulat-

ing the anisotropic stress-strain relations for poroelasticity in the compliance form, as we have also chosen to do. In contrast, while expressing the elastic material constants themselves in terms of compliances (*i.e.*, Young's modulus and Poisson's ratio), Loret *et al.*[42] have nevertheless emphasized the stiffness formulation of the poroelastic problem. But, in addition, they have also given careful consideration to relationships connecting the undrained and drained constants, as we have again chosen to do. However, these authors focus effort on somewhat different aspects of the problem than the more practical ones considered in the present work. In particular, their studies consider the issue of how to measure and/or estimate the quantities such as K_s and ϕ, which might be considered microscale quantities, especially if the solid material itself is *not* microhomogeneous,[6,21] as we have assumed it is in our measured samples. These issues are indeed important for a great many applications, but not so important for the data analysis we presented, since the samples we studied were in fact composed of very well-sorted materials. Thus, an assumption of microhomogeneity for these laboratory samples is quite reasonable. Such an assumption may not however always be equally good for field data in the earth, in ocean sediments, or in other applications of these methods. So the present analysis needs to be — and will be — subsequently generalized to incorporate these considerations pertaining to microheterogeneous frame materials in future work.

Acknowledgments

Work of both JGB and SN was performed under the auspices of the U.S. Department of Energy, at the Lawrence Berkeley National Laboratory under Contract No. DE-AC02-05CH11231. We thank Leon Thomsen for helpful comments on this work, and for finding some pertinent references to related and previously published (but nevertheless hard to find) work. Support was provided specifically by the Geosciences Research Program of the DOE Office of Basic Energy Sciences, Division of Chemical Sciences, Geosciences and Biosciences.

APPENDIX A: INVERTING A MATRIX FORMED FROM THE SUM OF AN INVERTIBLE MATRIX AND A RANK ONE MATRIX

A result used several times in the main text when we transform between compliance and stiffness matrices in poroelasticity involves the use of a fairly well-known fact about inverting simple matrix sums. The matrices of interest to us are always symmetric, so we use this condition here to simplify and shorten the discussion.

Suppose that we need to invert a matrix of the form:

$$\mathbf{M} = \mathbf{M}_0 + a\mathbf{n}\mathbf{n}^T, \tag{25}$$

where $\mathbf{M}_0$ is a square, invertible, $m \times m$ matrix, and $\mathbf{n}$ is a vector also of length m. The remaining variable a is a nonzero scalar, and for simplicity, we assume a is positive (although this condition is not always required). $\mathbf{M}_0$ is an invertible matrix by assumption, and $a\mathbf{n}\mathbf{n}^T$ is a rank-one matrix (having only one nonzero eigenvalue) regardless of the size of m as long as $m \geq 2$, and $a \neq 0$.

It turns out that the form of the matrix inverse of $\mathbf{M}$ must be:

$$\mathbf{M}^{-1} = \mathbf{M}_0^{-1} + b\mathbf{M}_0^{-1}\mathbf{n}\mathbf{n}^T\mathbf{M}_0^{-1}, \tag{26}$$

where b is a scalar to be determined. If the form (26) is correct, then multiplying (25) on the right (by symmetry, multiplying on the left produces the same final result) by (26) gives:

$$\mathbf{I} = \mathbf{I} + \left[a + b + ab\left(\mathbf{n}^T\mathbf{M}_0^{-1}\mathbf{n}\right)\right]\mathbf{n}\mathbf{n}^T\mathbf{M}_0^{-1}, \tag{27}$$

where $\mathbf{I}$ is an $m \times m$ identity matrix. Equation (27) shows — since the bracketed expression should vanish — that the previously unknown scalar b must satisfy:

$$b = -a/\left[1 + a\left(\mathbf{n}^T\mathbf{M}_0^{-1}\mathbf{n}\right)\right]. \tag{28}$$

Since, by assumption, $\mathbf{M}_0$ is invertible, and both a and $\mathbf{n}$ are known, this formula gives an explicit result for the scalar b, and therefore justifies the form of the inverse matrix assumed in (26).

Also note that this result was also used explicitly by Gassmann[21] in the final section (on anisotropic media) of his well-known paper on poroelasticity.

APPENDIX B: UNIAXIAL STRESS CONDITIONS AND THE UNIAXIAL EFFECTIVE STRESS COEFFICIENT X_3

For uniaxial stress conditions, we have $\sigma_{33} = -p_c$, $e_{11} = e_{22} = 0$, and in addition for the undrained case we have $\zeta = 0$. The transverse stresses $\sigma_{11} = \sigma_{22}$ are uncontrolled, but nevertheless determined by the boundary conditions. The fluid pressure is similarly determined by the system of equations, since the fluid is assumed to be undrained.

The pertinent equations for a transversely isotropic system are:

$$(s_{11} + s_{12})\sigma_{11} - s_{13}p_c + \beta_1 p_f = e_{11} = 0, \tag{29}$$

$$2s_{13}\sigma_{11} - s_{33}p_c + \beta_3 p_f = e_{33}, \tag{30}$$

and

$$-2\beta_1\sigma_{11} + \beta_3 p_c - \gamma p_f = -\zeta = 0, \tag{31}$$

with $e_{22} = e_{11}$ by symmetry, and similar statements about other symmetric variables and coefficients.

Equations (29) and (31) can be turned into a 2×2 system, and solved for σ_{11} and p_f as functions of p_c. The result of this process is:

$$\begin{pmatrix} -\sigma_{11} \\ p_f \end{pmatrix} = \begin{pmatrix} X_1 \\ X_2 \end{pmatrix} p_c, \tag{32}$$

where

$$X_1 = \frac{-s_{13}\gamma + \beta_1\beta_3}{(s_{11} + s_{12})\gamma - 2\beta_1^2} \quad \text{and} \quad X_2 = \frac{-2s_{13}\beta_1 + (s_{11} + s_{12})\beta_3}{(s_{11} + s_{12})\gamma - 2\beta_1^2}. \tag{33}$$

For this uniaxial system, X_2 clearly plays a role similar to that of Skempton's coefficient B in the isotropically confined case, giving the proportionality of pore pressure build up when confining pressure p_c increases. Also, the transverse stress σ_{11} build up is entirely analogous physically to $p_f = X_2 p_c$, but the proportionality constant is given instead by $-X_1$. (Note that we have chosen pressure p to be positive in compression, while stress σ is positive in tension – which is the reason for some of these minus signs.)

We can now define the correct effective stress for the uniaxial problem in the following way:

$$\frac{e_{33}}{-s_{33}} \equiv p_{eff} = \left[1 + \frac{2s_{13}}{s_{33}} X_1 - \frac{\beta_3}{s_{33}} X_2\right] p_c = [1 - X_3]\, p_c, \tag{34}$$

where the pertinent effective stress coefficient is therefore given by

$$X_3 \equiv \frac{2s_{13}^2\gamma - 4s_{13}\beta_1\beta_3 + (s_{11} + s_{12})\beta_3^2}{s_{33}\left[(s_{11} + s_{12})\gamma - 2\beta_1^2\right]}. \tag{35}$$

All the required coefficients in (35) except γ are drained constants (containing no factors of K_f), and so X_3 can be computed for the undrained experiments simply by using the earlier analysis in the main text of the present paper.

REFERENCES

[1]S. R. Pride and J. G. Berryman, "Connecting theory to experiment in poroelasticity," *Journal of the Mechanics and Physics Solids* **46**, 719–747 (1998).

[2]M. A. Biot, "Theory of propagation of elastic waves in a fluid-saturated porous solid. I. Low-frequency range," *J. Acoust. Soc. Am.* **28**, 168–178 (1956).

[3]M. A. Biot, "Theory of propagation of elastic waves in a fluid-saturated porous solid. II. Higher frequency range," *J. Acoust. Soc. Am.* **28**, 179–191 (1956).

[4]M. A. Biot and D. G. Willis, "The elastic coefficients of the theory of consolidation," *J. Appl. Mech.* **24**, 594–601 (1957).

[5]R. D. Stoll, "Acoustic waves in saturated sediments," in *Physics of Sound in Marine Sediments*, edited by L. Hampton, (Plenum, New York), pp. 19–39 (1974).

[6] R. J. S. Brown and J. Korringa, "On the dependence of the elastic properties of a porous rock on the compressiblity of the pore fluid," *Geophysics* **40**, 608–616 (1975).

[7]J. G. Berryman, "Confirmation of Biot's theory," *Applied Physics Letters* **37**, 382–384 (1980).

[8]G. Mavko and D. Jizba, "Estimating grain-scale fluid effects on velocity disperion in rocks," *Geophysics* **56**, 1940–1949 (1991).

[9]D. J. Hart and H. F. Wang, "Laboratory measurements of a complete set of poroelastic moduli for Berea sandstone and Indiana limestone," *Journal of Geophysical Research* (**100**), 17741–17751 (1995).

[10]J. G. Berryman, "Transversely isotropic elasticity and poroelasticity arising from thin isotropic layers," in *Theoretical and Computational Acoustics 1997*, edited by Y.-C. Teng and E.-C. Shang and Y.-H. Pao and M. H. Schultz and A. D. Pierce (World Scientific, Newark, NJ, 1997), pp. 457–474.

[11]J. G. Berryman (**1999**). "Origin of Gassmann's equations," *Geophysics* **64** (5), 1627–1629.

[12]B. T. Hefner and K. L. Williams, "Sound speed and attenuation measurements in unconsolidated glass-bead sediments saturated with viscous pore fluids," *J. Acoust. Soc.*

Am. **120** (5), 2538–2549 (2006).

[13]J. G. Berryman, "Seismic waves in rocks with fluids and fractures," *Geophysical Journal International* **40**, 608–616 (2007).

[14]X. Zhu and G. A. McMechan, "Direct estimation of the bulk modulus of the frame in a fluid-saturated elastic medium by Biot theory," in *60th International Meeting, Society of Exploration Geophysicists, Expanded Abstracts, 1990*, pp. 787–790.

[15] X. Zhu and G. A. McMechan, "Numerical simulation of seismic responses of poroelastic reservoirs using Biot theory," *Geophysics* **56** (3), 328–339 (1991).

[16] K. L. Williams, D. R. Jackson, E. I. Thorsos, D. Tang, and S. G. Schock, "Comparison of sound speed and attenuation measured in a sandy sediment to predictions based on the Biot theory of porous media," *IEEE J. Ocean. Eng.* **27**, 413–428 (2002).

[17]I. Ishibashi and O. F. Capar, "Anisotropy and its relation to liquefaction resistance of granular material," *Soils and Foundations* **43** (5), 149–159 (2003).

[18]C.-Y Wang., D. S. Dreger, C.-H. Wang, D. Mayeri, and J. G. Berryman, "Field relations among coseismic ground motion, water level change and liquefaction for the 1999 Chi-Chi earthquake," *Geophysical Research Letters*x **30** (17), 1980-1–1980-4 (2003).

[19]S. C. Cowin, "The significance of bone microstructure in mechanotransduction," *Journal of Biomechanics* **40** (S1), S105–S109 (2007).

[20] Y. J. Yoon and S. C. Cowin, "An estimate of anisotropic poroelastic constants of an osteon," *Biomechanics and Modeling in Mechanobiology* **7** (1), 1–11 (2008).

[21]F. Gassmann, "Über die Elastizität poröser Medien," *Vierteljahrsschrift der Naturforschenden Gesellschaft in Zürich*, **96**, 1–23 (1951).

[22]K. Lee, E. Park, and W. Seong, "High frequency measurements of sound speed and attenuation in water-saturated glass-beads of varying size," *J. Acoust. Soc. Am.* **126**, EL28–EL33 (2009).

[23]A. W. Wood, *A Textbook of Sound* (Bell, London, 1955), p. 360.

[24]A. Reuss, "Berechung der Fliessgrenze von Mischkristallen," *Z. Angew. Math. Mech.* **9**, 55 (1929).

[25]R. Hill, "The elastic behaviour of crystalline aggregate," *Proceedings of the Physical Society of London* **A65**, 349–354 (952).

[26]W. Voigt, *Lehrbuch der Kristallphysik*(Teubner, Leipzig, 1928), p. 962.

[27]A. W. Skempton, "The pore-pressure coefficients A and B," *Géotechnique* **4**, 143–147 (1954).

[28]D. Sherlock, K. Nihei, S. Nakagawa, and L. Duranti, "Stress-induced velocity anisotropy measurements in unconsolidated sand using a phased-array uniaxial compaction cell," *77th International Meeting, Society of Exploration Geophysicists, Expanded Abstracts, 2007*, **26**, 1550–1554.

[29]D. E. Miller and C. Spencer, "An exact inversion for anisotropic moduli from phase slowness data," *Journal of Geophysical Research* **99** (B11), 21651–21657 (1994).

[30]T. J. Plona, "Observation of a second bulk compressional wave in a porous medium at ultrasonic frequencies," *Applied Physics Letters* **36**, 259–261 (1980).

[31]R. C. Y. Chin, J. G. Berryman, and G. W. Hedstrom, "Generalized ray expansion for pulse propagation and attenuation in fluid-saturated porous media," *Wave Motion* **7**, 43–66 (1985).

[32]K. L. Williams, "An effective density fluid model for acoustic propagation in sediments derived from Biot theory," *J. Acoust. Soc. Am.* **110** (5), 2276–2281 (2001).

[33]N. P. Chotiros, "Biot model of sound propagation in water-saturated sand," *J. Acoust. Soc. Am.* **97** (1), 199–214 (1995).

[34] K. Walton (**1987**), "The effective elastic moduli of a random packing of spheres," *Journal of the Mechanics and Physics of Solids* **35**, 213–226 (1987).

[35]D. L. Johnson, L. M. Schwartz, D. Elata, J. G. Berryman, B. Hornby, and A. N. Norris, "Linear and nonlinear elasticity of granular media: Stress induced anisotropy of a random sphere pack," *ASME J. Appl. Mech.* **65**, 380–386 (1998).

[36]S. N. Domenico, "Elastic properties of unconsolidated porous reservoirs," *Geophysics* **42**, 1339–1368 (1977).

[37]W. F. Murphy III, *Effects of Microstructure and Pore Fluids on the Acoustic Properties*

of Granular Sedimentary Materials, Ph.D. thesis, Stanford University, Stanford, California, 1982.

[38]M. A. Zimmer, M. Prasad, G. Mavko, and A. Nur, "Seismic velocities of unconsolidated sands: Part 1 — Pressure trends from 0.1 to 20 MPa," *Geophysics* **72**, E1–E13 (2007).

[39]B. Gurevich, D. Makarynska, and M. Pervukhina, "Ultrasonic moduli for fluid-saturated rocks: Mavko-Jizba relations rederived and generalized," *Geophysics* **74**, N25–N30 (2009).

[40]M. Thompson and J. R. Willis, "A reformation of the equations of anisotropic poroelasticity," *ASME Journal of Applied Mechanics*, **58**, 612–616 (1991).

[41]S. C. Cowin, "Anisotropic poroelasticity: Fabric tensor formulation," *Mechanics of Materials* **36** (8), 665–677 (2004).

[42]B. Loret, E. Rizzi, and Z. Zerfa, "Relations between drained and undrained moduli in anisotropic poroelasticity," *Journal of the Mechanics and Physics of Solids* **49** (11), 2593–2619 (2001).

LIST OF FIGURES